Maximum Orbit Plane Change with Heat-Transfer-Rate Considerations

J. Y. Lee* and D. G. Hull†
University of Texas at Austin, Austin, Texas 78712

Two aerodynamic maneuvers are considered for maximizing the plane change of a circular orbit; gliding flight with a maximum thrust segment to regain lost energy (aeroglide) and constant altitude cruise with the thrust being used to cancel the drag and maintain a high energy level (aerocruise). In both cases, the stagnation heating rate is limited. For aeroglide, the controls are the angle of attack, the bank angle, the time at which the burn begins, and the length of the burn. For aerocruise, the maneuver is divided into three segments: descent, cruise, and ascent. During descent the thrust is zero, and the controls are the angle of attack and the bank angle. During cruise, the only control is the assumed-constant angle of attack. During ascent, a maximum thrust segment is used to restore lost energy, and the controls are the angle of attack and bank angle. The optimization problems are solved with a nonlinear programming code known as GRG2. Numerical results for the Maneuverable Re-entry Research Vehicle with a heating-rate limit of 100 Btu/ft²-s show that aerocruise gives a maximum plane change of 23 deg, which is only 1 deg larger than that of aeroglide. On the other hand, even though aerocruise requires two thrust levels, the cruise characteristics of constant altitude, velocity, thrust, and angle of attack are easy to control.

Nomenclature

C = specific mass flow rate, slugs/s-lb
C_D = drag coefficient
C_L = lift coefficient
c = engine characteristic velocity, ft/s
D = drag, lb
g = acceleration of gravity, ft/s²
H = Hamiltonian function
h = altitude, ft
i = inclination angle
L = lift, lb
m = mass, slugs
m_e = empty mass, slugs
m_f = mass after plane change accomplished, slugs
$\dot{Q}$ = heat-transfer rate, Btu/ft²-s
$\dot{Q}_r$ = reference heat-transfer rate, Btu/ft²-s
r = distance from center of earth to vehicle, ft
S_R = aerodynamic reference area, ft²
T = thrust, lb
t = time, s
t_B = engine ignition time, s
t_{BO} = engine burnout time, s
t_f = time at the end of ascent, s
t_1 = time at the end of descent, s
t_2 = time at the end of aerocruise, s
V = velocity, ft/s
ΔV_1 = deorbit impulse, ft/s
ΔV_2 = boost impulse, ft/s
ΔV_3 = reorbit impulse, ft/s
α = angle of attack
γ = flight-path angle
θ = longitude
λ = Lagrange multiplier
μ = bank angle
$\bar{\mu}$ = gravitational constant of Earth, ft³/s²
ρ = density, slugs/ft³
ϕ = latitude
ψ = heading angle

Subscripts
c = circular orbit
f = final, end of atmospheric flight
o = initial, beginning of atmospheric flight
s = sea level

Introduction

FOR aeroassisted, orbit-plane-change maneuvers, two types of atmospheric flight have been studied: aeroglide and aerocruise. In aeroglide, gliding flight is combined with a maximum thrust segment to accomplish the orbit transfer; in aerocruise, however, a continuous thrust is applied to cancel drag and maintain a high velocity.

Without considering the heating constraint, many studies have shown that aeroglide and aerocruise are much better than extra-atmospheric plane-change maneuvers, and aerocruise is the superior mode for large plane changes (e.g., greater than 15 deg).[1,2]

Actually, all structural materials have the limitation of maximum heat endurance; therefore, a heating constraint should be considered in the aeroassisted plane-change maneuver. Only a few studies can be found that include a heating constraint.[3-5] In Ref. 4, Clauss and Yeatman show that the heating constraint substantially reduces the synergetic orbit plane-change performance, and the reduction is more severe for aeroglide than for aerocruise. Dickmanns[5] develops numerical solutions for the synergetic plane-change problem for a vehicle whose angle of attack, bank angle, thrust magnitude, thrust angle of attack, and thrust sideslip angle can be controlled. The heat transfer constraint depends on the angle of attack, and only the atmospheric portion of the maneuver is considered. For the Maneuverable Re-entry Research Vehicle (MRRV) without a heating constraint,[6] aeroglide can change the plane of a 100 n.mi. circular orbit 34 deg. With a heating constraint, only aerocruise has been considered.[7]

Received July 21, 1988; revision received Dec. 19, 1988.

*Graduate Student, Department of Aerospace Engineering and Engineering Mechanics; currently, Associate Scientist, CSIST, Taiwan, ROC.

†M. J. Thompson Regents Professor, Department of Aerospace Engineering and Engineering Mechanics. Associate Fellow AIAA.

In this paper, the maximum plane change is determined first for aeroglide and then for aerocruise. Aerodynamic heating is included by constraining the heating rate to be less than 100 Btu/ft^2-s at the stagnation point. The problem is formulated as a parameter optimization problem and is solved by the nonlinear programming code GRG2.[8]

Physical Model

In this paper, the problem of maximizing the plane change of a 100 n.mi. circular orbit using the MRRV is solved. The orbit transfer maneuver is composed of a deorbit impulse followed by a coast to atmosphere entry (60 n.mi.), a hypersonic turn in the atmosphere (aeroglide or aerocruise), an impulse at atmosphere exit to boost the vehicle to orbit altitude, and an impulse at apogee to reestablish the circular orbit. All of the impulses are along the vehicle velocity vector so that the entire plane change takes place in atmosphere. In the following paragraphs, the physical model for this problem (the Earth and its atmosphere, the vehicle, the equations of motion, and the stagnation point heating rate) is discussed briefly; a detailed description, including values for all physical parameters, is contained in Ref. 6.

Earth and Atmosphere

The Earth is assumed to be a nonrotating sphere whose radius r_s represents mean sea level, and the acceleration of gravity is given by the inverse square law. The atmosphere model is the 1962 U.S. Standard Atmosphere whose properties are functions of altitude only.

Vehicle

The vehicle for this study is the MRRV developed by the Air Force Flight Dynamics Laboratory. Its aerodynamic and mass characteristics are presented in Ref. 6. It is interesting to note that as the altitude increases, the maximum lift-to-drag ratio, $E_{\max}$, decreases, but the angle of attack at $E_{\max}$ increases. For $h = 240$ kft, $E_{\max}$ is 2.04 at an angle of attack of 16 deg. The angle of attack is limited to 40 deg. The vehicle can produce up to 3300 lb of thrust with a specific mass flow rate of 1.054 E-4 slugs/s-lb. To calculate mass changes during impulses, the characteristic velocity of the engine is arbitrarily chosen to be $c = 10{,}000$ ft/s.

Equations of Motion

The system of equations of motion includes deorbit equations, atmospheric flight equations, and boost-and-reorbit equations.

Deorbit Equations

Deorbit is accomplished by an impulse ΔV_1, which causes the vehicle to enter the atmosphere at radius r_o with velocity V_o and flight-path angle γ_o from the circular orbit of radius r_c with velocity V_c. From the conservation of energy and angular momentum, V_o and γ_o can be expressed as follows[9]:

$$V_o = [(V_c - \Delta V_1)^2 - 2\bar{\mu}(1/r_c - 1/r_o)]^{1/2} \tag{1}$$

$$\gamma_o = -\cos^{-1}[(V_c - \Delta V_1)/r_o V_o] \tag{2}$$

where $\bar{\mu}$ is the gravitational constant. In order to insure atmospheric entry, ΔV_1 must satisfy the relation

$$\Delta V_1 \geq \Delta V_{1_{\min}} = V_c - \left\{2(V_c^2 - \bar{\mu}/r_o)/[1 - (r_c/r_o)^2]\right\}^{1/2} \tag{3}$$

Because of the impulse, the mass of the vehicle at atmosphere entry is given by

$$m_o = m_c \exp(-\Delta V_1/c) \tag{4}$$

where c is the characteristic velocity of the engine.

Atmospheric Flight Equations

The vehicle is assumed to fly over a nonrotating spherical Earth (Fig. 1). If the vehicle is moving from west to east, and if a positive bank angle generates a heading toward the north, the equations of motion are as follows:

$$\dot{\theta} = V \cos\gamma \cos\psi/(r \cos\phi) \tag{5}$$

$$\dot{\phi} = V \cos\gamma \sin\psi/r \tag{6}$$

$$\dot{r} = V \sin\gamma \tag{7}$$

$$\dot{V} = (T \cos\alpha - D)/m - g \sin\gamma \tag{8}$$

$$\dot{\gamma} = (T \sin\alpha + L) \cos\mu/(mV) + (V^2/r - g) \cos\gamma/V \tag{9}$$

$$\dot{\psi} = (T \sin\alpha + L) \sin\mu/(mV \cos\gamma) - (V/r) \cos\gamma \cos\psi \tan\phi \tag{10}$$

$$\dot{m} = -CT \tag{11}$$

where θ is the longitude, ϕ the latitude, $r = r_s + h$ the radial distance from the center of the Earth to the vehicle center of mass, h the altitude, V the velocity, γ the flight-path angle, ψ the heading angle, m the mass, T the thrust, C the specific mass flow rate, D the drag, L the lift, α the angle of attack, and μ the bank angle. Lift L and drag D are defined as

$$L = \tfrac{1}{2}\rho V^2 C_L(\alpha, M, h) S_R, \qquad D = \tfrac{1}{2}\rho V^2 C_D(\alpha, M, h) S_R \tag{12}$$

where ρ is the density of the atmosphere, M is the Mach number, and S_R is the aerodynamic reference area. During atmospheric flight, the controls are the angle of attack, bank angle, and thrust.

Boost and Reorbit Equations

The vehicle exits the atmosphere at $r_f = r_o$, V_f, and γ_f. At this point, the impulse ΔV_2 is applied to raise the apogee of the ascending elliptical orbit to r_c. Then, a final impulse ΔV_3 is used to increase the velocity to V_c. By applying the conservation of energy and angular momentum, expressions for ΔV_2 and ΔV_3 are[9]

$$\Delta V_2 = \left[\frac{2\bar{\mu}(1/r_f - 1/r_c)}{1 - (r_f/r_c)^2 \cos^2\gamma_f}\right]^{1/2} - V_f \tag{13}$$

$$\Delta V_3 = V_c - \frac{r_f}{r_c}\left[\frac{2\bar{\mu}(1/r_f - 1/r_c)}{1 - (r_f/r_c)^2 \cos^2\gamma_f}\right]^{1/2} \cos\gamma_f \tag{14}$$

Finally, the mass of the vehicle in orbit is

$$m_f' = m_f \exp(-\Delta V_2/c) \exp(-\Delta V_3/c) = m_f'(r_f, V_f, \gamma_f, m_f) \tag{15}$$

and is a function only of the conditions at atmosphere exit.

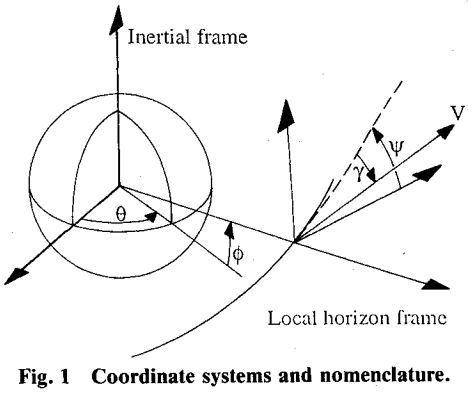

Fig. 1 Coordinate systems and nomenclature.

Stagnation Point Heating Rate

Many different heating constraints have been used for a vehicle.[5,7,9] In Ref. 10, three heating constraints are considered: reference (by Chapman's equation), stagnation point, and windward-centerline heating rate. In this study, the stagnation point heating is considered. The stagnation point heat transfer rate is expressed as[10]

$$\dot{Q} = 17600(\rho/\rho_s)^{0.5}(V/\overline{V}_s)^{3.15} \tag{16}$$

where ρ_s is the density of the atmosphere at sea level and $\overline{V}_s$ is the orbital velocity at sea level.

General Formulation of Optimal Plane-Change Problem

The optimal control problem can be formulated in terms of the atmospheric part of the orbit transfer maneuver. The performance index is the plane change of a 100 n.mi. circular orbit. For a nonrotating Earth, the plane change is given by [6]

$$i_f = \cos^{-1}(\cos\psi_f \cos\phi_f) \tag{17}$$

The vehicle motion is governed by the differential Eqs. (5-11) where the control variables are the angle of attack, the bank angle, and the thrust. The prescribed initial conditions are written as

$$\theta_o = 0, \quad \phi_o = 0 \quad h_o = 60 \text{ n.mi.}, \quad V_o = V_o(\Delta V_1)$$
$$\gamma_o = \gamma_o(\Delta V_1), \quad \psi_o = 0, \quad m_o = m_o(\Delta V_1) \tag{18}$$

where ΔV_1 must satisfy the inequality constraint

$$\Delta V_1 - V_c + \left\{2(V_c^2 - \bar{\mu}/r_o)/[1-(r_c/r_o)^2]\right\}^{1/2} \geq 0 \tag{19}$$

The final condition is

$$h_f = 60 \text{ n.mi.} \tag{20}$$

To insure that the vehicle is leaving the atmosphere and to insure that the mass of the vehicle reaching orbit is not less than the empty weight, the following inequality constraints are imposed:

$$\gamma_f \geq 0 \tag{21}$$

$$m_f'(r_f, V_f, \gamma_f, m_f) - m_e \geq 0 \tag{22}$$

where m_f' is defined by Eq. (15), and m_e is the empty mass.

Next, the controls are subject to the control variable inequality constraints

$$5 \leq \alpha \leq 40 \text{ deg}, \quad 0 \leq \mu \leq 180 \text{ deg}, \quad 0 \leq T \leq 3300 \text{ lb} \tag{23}$$

where the lower bound on α insures that $C_L > 0$. Finally, the heating rate constraint has the form

$$\dot{Q}(r, V) \leq \dot{Q}_r = 100 \text{ Btu/ft}^2\text{-s} \tag{24}$$

which is a state variable inequality constraint.

The problem is reduced to a suboptimal control problem or, equivalently, a parameter optimization problem and solved by the nonlinear programming code GRG2.[8] First, the heating constraint $\dot{Q} \leq \dot{Q}_r$ is converted to a penalty function by introducing the new variable $y(t)$ defined as

$$\dot{y} = -\min^2[1-(\dot{Q}/\dot{Q}_r), 0], \quad y_o = 0 \tag{25}$$

adding another differential equation and initial condition. The heating constraint becomes

$$y_f \geq 0 \tag{26}$$

In GRG2, the control variable inequality constraints are handled as direct bounds on the control nodes. Second, the problem is converted to a fixed final time problem by introducing a new independent variable $\tau = t/t_f$; this causes t_f to be a parameter. Third, each time-distributed control function is replaced by a set of equally spaced nodal points over the normalized time interval [0,1], and linear interpolation is used to form the control function.

The unknown parameters in the preceding problem formulation are the impulse ΔV_1, the final time t_f, and the control nodes for α, μ, and T. If values are given for these parameters, the differential equations (5-11) and (25) can be integrated from $\tau_o = 0$ and the initial conditions [Eqs. (18) and (25)] to the final time $\tau_f = 1$. Then, with the resulting final states, the performance index (17), the equality constraint (20), and the inequality constraints (19), (21), (22), and (26) can be calculated. If X denotes the vector of parameters, the nonlinear programming problem is stated as follows: minimize the performance index

$$F(X) \equiv -i_f \tag{27}$$

subject to the equality constraint

$$G(X) \equiv h_f - 60 \text{ n.mi.} = 0 \tag{28}$$

and the inequality constraints

$$H(X) \equiv \begin{bmatrix} \Delta V_1 - \Delta V_{1_{\min}} \\ \gamma_f \\ m_f' - m_e \\ y_f \end{bmatrix} \tag{29}$$

A fixed-step, fourth-order Runge-Kutta integrator is used to integrate the differential equations. To improve the convergence, nondimensional equations are used, and all the parameters and the constraint functions are scaled to order 1. In addition, the derivatives of the performance index and the constraint functions with respect to the parameters are calculated by a central difference algorithm provided by GRG2, and the perturbation ratio is 10^{-4}. The convergence tolerance is also taken to be 10^{-4}. All the calculations in this study are done by the CDC Dual Cyber 170/750 at the University of Texas at Austin.

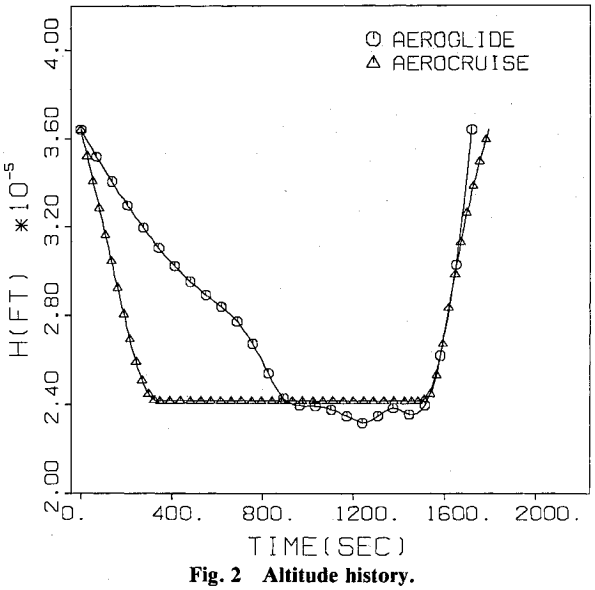

Fig. 2 Altitude history.

In the following section, two different strategies are used for the atmospheric part of the orbit transfer maneuver: aeroglide and aerocruise.

Aeroglide

This strategy involves gliding flight ($T=0$) in the atmosphere combined with a maximum thrust ($T=3300$ lb) segment to restore lost energy. The times at which the engines are turned on (t_B) and turned off (t_{BO}) become parameters to be optimized. For this problem, the parameters are the first impulse ΔV_1, the final time t_f, 11 node points for α, 11 node points for μ, the burn time t_B, and the burnout time t_{BO}.

The number of integration steps is 250. In addition, t_B and t_{BO} usually occur within an integration step. During that step, two partial integration steps are taken.

Numerical results for the altitude, heat-transfer rate, angle of attack, bank angle, velocity, and inclination angle histories are shown in Figs. 2–7. Useful data are as follows:

$$t_B = 1222.7 \text{ s}, \quad t_{BO} = 1690.385 \text{ s}, \quad t_f = 1719.8 \text{ s}$$

$$\theta_f = 114.9 \text{ deg}, \quad \phi_f = 9.55 \text{ deg}, \quad \psi_f = 19.83 \text{ deg}$$

$$i_f = 21.93 \text{ deg}, \quad \Delta V_1 = 100.581 \text{ ft/s}, \quad \Delta V_2 = 0.197 \text{ ft/s}$$

$$\Delta V_3 = 812.040 \text{ ft/s}, \quad \gamma_o = -0.4 \text{ deg}, \quad V_o = 25{,}770 \text{ ft/s}$$

$$\gamma_f = 2.11 \text{ deg}, \quad V_f = 25{,}067 \text{ ft/s} \tag{30}$$

and additional data are presented in Ref. 12. Note that the required reboost impulse is essentially zero.

Figures 2–7 show that significant events occur around 400, 800, and 1200 s. For the first 400 s of the trajectory, the vehicle is operating at $\alpha = 40$ deg and $\mu \approx 65$ deg; the altitude continues to decrease, and the velocity stays approximately constant. Around 400 s, atmospheric forces begin to affect the trajectory; the angle of attack is decreased to increase the lift-to-drag ratio; and the bank angle is increased to move the vehicle deeper into the atmosphere. As the heating boundary is approached, the angle of attack is returned to 40 deg, and the bank angle is decreased to around 60 deg. During this time, the velocity remains nearly constant.

The heating boundary is encountered at around 800 s into the atmosphere at an altitude of approximately 240 kft and is held until 1200 s. The altitude decreases slightly, and the entire velocity decrease occurs during this time. Again, the angle of attack decreases to increase the lift-to-drag ratio, whereas the bank angle is nearly constant. As the engine ignition time is approached, the angle of attack returns to 40 deg.

At approximately 1200 s, the engines begin producing thrust. From 1200 to 1600 s, the altitude and velocity remain

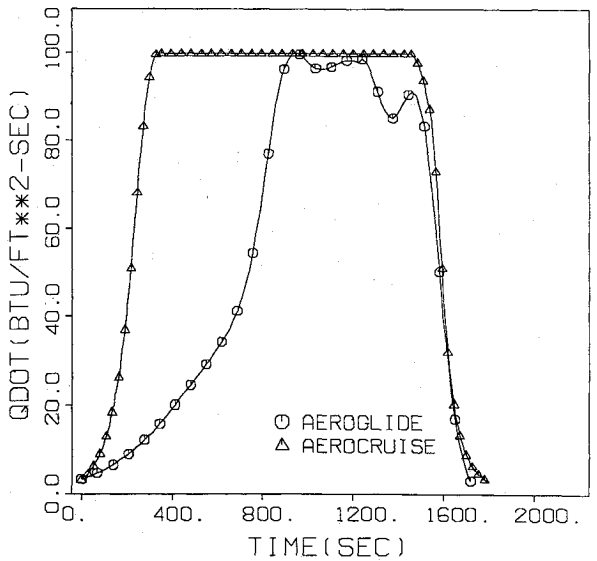

Fig. 3 Heat-transfer-rate history.

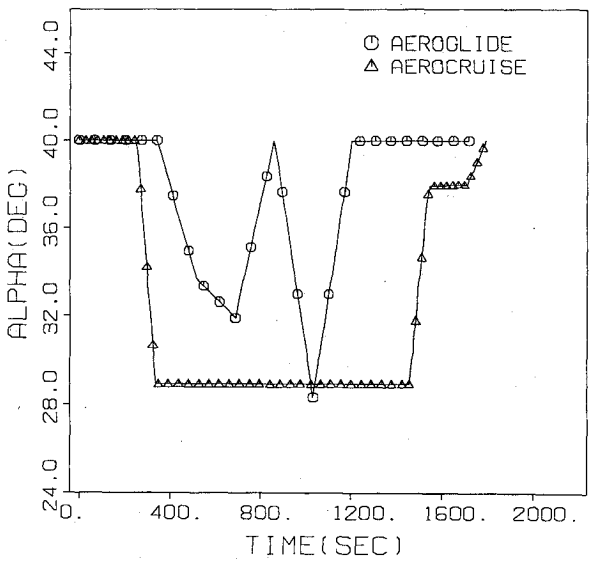

Fig. 4 Angle-of-attack history.

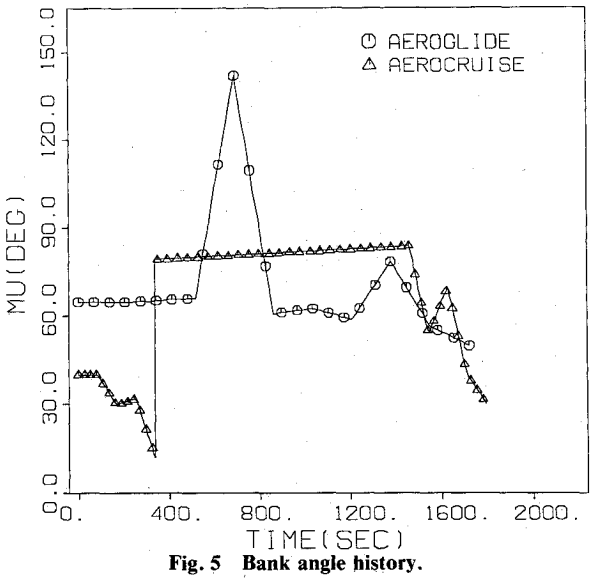

Fig. 5 Bank angle history.

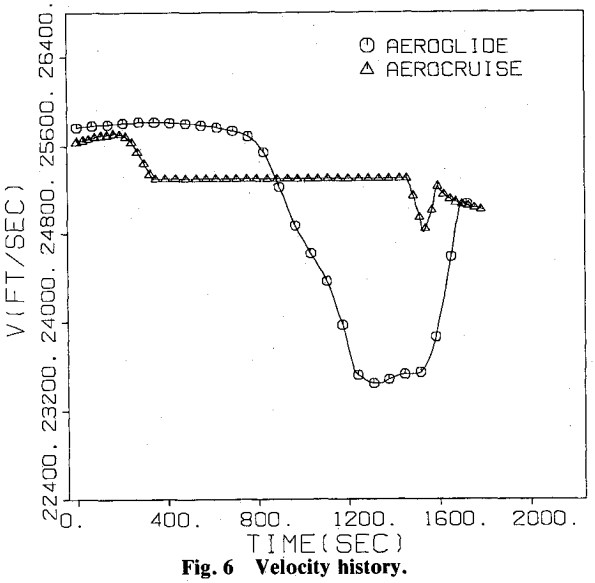

Fig. 6 Velocity history.

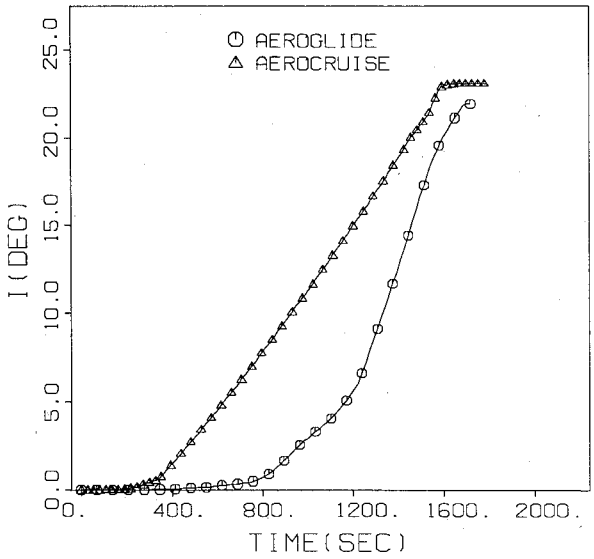

Fig. 7 Inclination angle history.

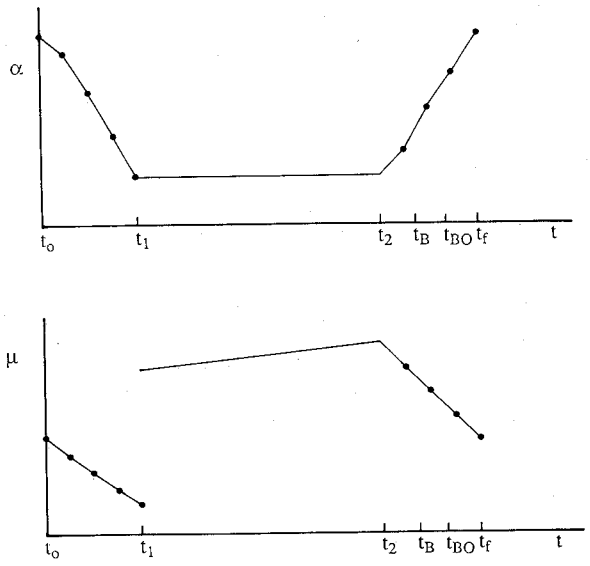

Fig. 8 Assumed nodes for each control history.

fairly constant. The angle of attack is held at 40 deg, and the bank angle is increased to nearly 80 deg so that the thrust can contribute as much as possible to achieving plane change. Then, as it becomes necessary to leave the atmosphere, the bank angle is decreased in order to increase the upward component of the thrust. During this time, the altitude and the velocity increase rapidly.

Figure 7 shows that approximately 6 deg of plane change is achieved while on the heating boundary and that an approximately 16 deg change occurs when operating at maximum thrust. Prior to 800 s, almost no plane change occurs.

Aerocruise

In the aerocruise orbit transfer maneuver, the atmospheric part is divided into three stages. The first stage is a descent stage in which $T=0$ and the controls are α and μ. During this stage, the vehicle descends to and makes a transition into the cruise stage. The second stage is the cruise stage in which $T\cos\alpha = D$ and the control is α. This stage is discussed in more detail in the next paragraph. The third stage is the ascent stage in which $T=0$ and the controls are α and μ. During this stage, a maximum thrust segment is allowed to remove any energy deficiency.

To make the cruise stage as efficient as possible, it should be as deep in the atmosphere as possible to obtain a high density. Since the heating boundary limits this altitude, the cruise segment should be the heating boundary. If the thrust cancels the drag ($T\cos\alpha = D$), the equation of motion (8) shows that $\gamma<0$ gives $\dot{V}>0$, and Eq. (16) implies that $\dot{Q}>0$. Also, $\gamma>0$ gives $\dot{V}<0$, and $\dot{Q}<0$. The only way to fly at $\dot{Q}=$ const is to fly at $\gamma=0$, which implies that $\dot{V}=0$. Hence, the cruise should be flown at constant altitude and constant velocity.

Studies of such a cruise (for example, Ref. 13) have shown that the angle of attack is nearly constant. Hence, to simplify the cruise as much as possible, the angle of attack is assumed constant, but its optimal value is to be determined. Since the drag and lift coefficients are now constants, the cruise is characterized by constant drag, constant lift, and constant thrust.

The equations of motion for the descent and ascent stages are the same as before. Those for the cruise stage are modified to include the characteristic of constant altitude ($r=$ const) and constant velocity and are given by

$$\dot{\theta} = V\cos\psi/r\cos\phi \tag{31}$$

$$\dot{\phi} = V\sin\psi/r \tag{32}$$

$$\dot{\psi} = (T\sin\alpha + L)\sin\mu/mV - V\cos\psi\tan\phi/r \tag{33}$$

$$\dot{m} = -CT \tag{34}$$

where the flight-path angle equation (9) determines the bank angle as a function of the angle of attack, that is,

$$\mu = \cos^{-1}\left[\frac{m(g-V^2/r)}{T\sin\alpha + L}\right] \tag{35}$$

Since all the states must be continuous at the junctions of adjacent stages, the initial conditions of the second stage must be the final conditions of the first stage. Hence, the altitude and the velocity of the cruise are those at the end of the descent. Then, to satisfy continuity for the flight-path angle, the condition

$$\gamma_1 = 0 \tag{36}$$

must be imposed at the end of the descent, that is, at time t_1. At the second junction, between cruise and ascent at time t_2, the initial states for ascent are taken to be the final states of the cruise.

The assumed forms of the control histories are shown in Fig. 8. During the descent stage, there are five nodes for α and five nodes for μ (equally spaced). During the cruise stage, the angle of attack is taken to be the value at the end of descent, and the bank angle is given by Eq. (35). Hence, there must be a discontinuity in μ at t_1. At t_2, the angle of attack and the bank angle are made continuous so that there are only four equally spaced nodes for each control during the ascent stage.

The remaining parameters in the problem are the times at the end of each stage (t_1, t_2, t_f) and the burn times of the maximum thrust segment in the ascent stage (t_B, t_{BO}). With the nine nodes for α, the nine nodes for μ, and the deorbit impulse ΔV_1, the total number of elements in the parameter vector X is 24.

Given values for each of these parameters, that is, given X, the equations of motion for each segment and Eq. (25) can be integrated to obtain the final states and values for the performance index and all of the constraints. The nonlinear programming problem has the same form as Eqs. (27–29), but Eq. (28) is to be replaced by

$$h(X) \equiv \begin{bmatrix} \gamma_1 \\ h_f - 60 \text{ n.mi.} \end{bmatrix} = 0 \tag{37}$$

In the integration of the differential equations, the time is normalized in each stage, and the time transformations are given by

$$\tau = t/t_1 \tag{38a}$$

$$\tau = (t-t_1)/(t_2-t_1) \tag{38b}$$

$$\tau = (t-t_2)/(t_f-t_2) \tag{38c}$$

The number of integration steps is 100 for descent and ascent and 200 for cruise.

Complete numerical results are presented in Ref. 12. Here, altitude, heat transfer rate, angle of attack, bank angle, velocity, and inclination angle are presented in Figs. 2-7. Additional data are as follows:

$t_1 = 337.4$ s, $t_2 = 1463.8$ s, $t_f = 1800.9$ s

Cruise: $V = 25{,}305$ ft/s, $h = 241{,}940$ ft, $T = 1149.3$ lb

$\theta_f = 122.3$ deg, $\phi_f = 18.21$ deg, $\psi_f = 14.33$ deg

$i_f = 23.02$ deg, $\Delta V_1 = 231.1$ ft/s, $\Delta V_2 = 705.8$ ft/s

$\Delta V_3 = 168.1$ ft/s, $\gamma_o = -0.96$ deg, $V_o = 25{,}641$ ft/s

$\gamma_f = 0.74$ deg, $V_f = 24{,}997$ ft/s, $t_B = 1536$ s, $t_{BO} = 1668$ s

It is noted in Fig. 2 that the vehicle descends rapidly to the optimal cruise altitude of 242,000 ft, cruises for 1126 s, and ascends rapidly to the boundary of the atmosphere. During the cruise, the trajectory is on the heating boundary (Fig. 3). The angle of attack (Fig. 4) during descent is 40 deg, and as the cruise is approached, it decreases to the cruise value of 29 deg. During ascent, the angle of attack returns to around 40 deg. On descent, the bank angle decreases to roll the lift vector upward to transition to cruise (Fig. 5). On ascent, the bank angle decreases so that the increased upward component of the lift can take the vehicle out of the atmosphere. In this stage, there is a maximum thrust burn for 132.2 s. Note the increase in μ during this time to get additional plane change. This burn is also visible in the velocity figure (Fig. 6). Most of the plane change occurs during cruise. However, over a 1 deg of plane change occurs during the maximum thrust segment (Fig. 7).

Discussion and Conclusions

Two strategies, aeroglide and aerocruise, have been considered for the atmospheric part of an aeroassisted, orbital, plane-change maneuver: 1) gliding flight with a maximum thrust segment to restore lost energy and 2) a rapid descent to a constant altitude, constant velocity, constant angle-of-attack cruise followed by an ascent with a maximum thrust segment to add energy. In each case, the stagnation point heating rate is limited.

The maximum plane change for aeroglide ($i_f = 22$ deg) is only 1 deg less than that for aerocruise ($i_f = 23$ deg). In the aeroglide maneuver, the boost impulse is not required, whereas it is for the aerocruise maneuver. If this burn had been required to be a part of the maximum thrust segment during the ascent stage (to reduce the number of burns), the plane change achieved by the aerocruise maneuver would be reduced. Then, aeroglide and aerocruise would produce about the same plane change. From a guidance point of view, aerocruise seems to be a better baseline maneuver because most of the states and controls are constant.

The cruise portion of the aerocruise maneuver has been studied by itself in a number of papers. Here, however, the entire orbit transfer maneuver has been considered.

Acknowledgment

This research was supported in part by the NASA Jet Propulsion Laboratory through Contract NAS 7-100, managed by K. D. Mease and L. J. Wood.

References

[1]London, H. S., "Change of Satellite Orbit Plane by Aerodynamic Maneuvering," *The Journal of Aerospace Sciences,* Vol. 29, No. 3, 1962, pp. 323-332.

[2]Cuadra, E., and Arthur, D., "Orbit Plane Change by External Burning Aerocruise," *Journal of Spacecraft and Rockets,* Vol. 3, No. 3, 1966, pp. 341-362.

[3]Lau, J., "Implications of Maneuvering-Range Constraints on Lifting-Vehicle Design," *Journal of Spacecraft and Rockets,* Vol. 4, No. 5, 1967, pp. 639-643.

[4]Clauss, J. S., Jr., and Yeatman, R. D., "Effect of Heating Restraints on Aeroglide and Aerocruise Synergetic Maneuver Performance," *Journal of Spacecraft and Rockets,* Vol. 4, No. 8, 1967, 1107-1109.

[5]Dickmanns, E. D., "The Effect of Finite Thrust and Heating Constraints on the Synergetic Plane Change Maneuver for a Space Shuttle Orbiter-Class Vehicle," NASA TN D-7211, Oct. 1973.

[6]Hull, D. G., and Speyer, J. L., "Optimal Reentry and Plane-Change Trajectories," *The Journal of the Astronautical Sciences,* Vol. 30, No. 2, 1982, pp. 117-130.

[7]Ikawa, H., and Rudiger, T. F., "Synergetic Maneuvering of Winged Spacecraft for Orbital Plane Change," *Journal of Spacecraft and Rockets,* Vol. 19, No. 6, 1982, pp. 513-520.

[8]Lasdon, L. S., and Waren, A. D., "Generalized Reduced Gradient Software for Linearly and Nonlinearly Constrained Problems," Dept. of General Business, Univ. of Texas at Austin, Austin, TX, working paper 77-85, 1977.

[9]Hull, D. G., Giltner, J. M., Speyer, J. L., and Mapar, J., "Minimum Energy-Loss Guidance for Aeroassisted Orbital Plane Change," *Journal of Guidance, Control, and Dynamics,* Vol. 8, No. 4, 1985, pp. 487-493.

[10]Wurster, K. E., and Eldred, C. H., "Technology and Operational Considerations for Low-Heat-Rate Entry Trajectories," *Journal of Spacecraft and Rockets,* Vol. 17, No. 5, 1980, pp. 459-464.

[11]Braver, G. L., Cornick, D. E., Habeger, A. R., Peterson, F. M., and Stevenson., R., "Program to Optimize Simulated Trajectories (POST) Volume I - Formulation Manual," NASA CR-132689, April 1975.

[12]Lee, J.- Y., "Manimum Orbit Plane Change with Heat-Transfer-Rate Considerations," Ph.D. Dissertation, Univ. of Texas at Austin, Austin, TX, May 1988.

[13]Mease, K. D., Lee, J., and Vinh, N. X., "Orbital Changes During Hypervelocity Aerocruise," *The Journal of the Astronautical Sciences,* Vol. 36, Nos. 1/2, 1988, pp. 103-137.